



A dual functional fluorescent probe for glioma imaging mediated by Blood-brain barrier penetration and glioma cell targeting



Hongwei Ma^{a,d,1}, Zhiyong Gao^{b,1}, Panfeng Yu^c, Shun Shen^e, Yongmei Liu^{f,*}, Bainan Xu^{a,*}

^a Department of Neurosurgery, Chinese PLA General Hospital, No. 28 Fuxing Road, Beijing 100853, PR China

^b Department of anesthesiology, Aviation Industry of China 363 Hospital, Chengdu 610041, PR China

^c Department of Orthopaedics, Chinese Air Force General Hospital, No. 30 Fucheng Road, Beijing 100142, PR China

^d School of Pharmacy, Fudan University, No. 826 Zhangheng Road, Shanghai 201203, PR China

^e Department of Neurosurgery, Chinese Air Force General Hospital, No. 30 Fucheng Road, Beijing 100142, PR China

^f Department of Thoracic Oncology, Cancer center, West China Hospital, Sichuan University, Chengdu 610041, PR China

ARTICLE INFO

Article history:

Received 22 April 2014

Available online 4 May 2014

Keywords:

AS1411 aptamer

TGN peptide

Glioma

Non-invasive imaging

ABSTRACT

Glioma is a huge threat for human being because it was hard to be completely removed owing to both the infiltrating growth of glioma cells and integrity of blood brain barrier. Thus effectively imaging the glioma cells may pave a way for surgical removing of glioma. In this study, a fluorescent probe, Cy3, was anchored onto the terminal of AS1411, a glioma cell targeting aptamer, and then TGN, a BBB targeting peptide, was conjugated with Cy3-AS1411 through a PEG linker. The production, named AsT, was characterized by gel electrophoresis, ¹H NMR and FTIR. In vitro cellular uptake and glioma spheroid uptake demonstrated the AsT could not only be uptaken by both glioma and endothelial cells, but also penetrate through endothelial cell monolayer and uptake by glioma spheroids. In vivo, AsT could effectively target to glioma with high intensity. In conclusion, AsT could be used as an effective glioma imaging probe.

© 2014 Elsevier Inc. All rights reserved.

1. Introduction

Brain tumor is an increasingly serious threat for human being. Among all original brain tumors, glioma accounts for 80% and is characterized by high mortality [1]. Due to the infiltration growth of glioma cells, completely removing glioma cells by surgery is an impossible mission and the reserved glioma cells often, if not absolutely, lead to recurrence. Although surgery resection followed with chemotherapy/radiotherapy may expand the median survival time, it still is restricted at approximately 15 months [2]. Thus accurate imaging of glioma cells is urgent for complete removing of glioma cells by surgery, which may decrease the recurrence rate and further improve life span of glioma bearing patients.

At present, fluorescent imaging-aid surgical resection of tumor cells has been come into reality in peripheral tumor [3]. However, these imaging probes could not be used for glioma cells imaging because of the infiltrated growth of glioma cells and the integrity of blood brain barrier (BBB) in the infiltrated area which restricted the distribution of these probes from blood to brain and brain glioma [4]. To conquer this barrier and specific target to glioma cells,

probes must be recognized by both BBB and glioma cells. Fortunately, there are many receptors that overexpressed on BBB or glioma cells, which ligands were often used in glioma targeting delivery. TGN is a peptide that selected from a library by phage display, which showed high BBB targeting efficiency and has been used for brain targeting delivery with well outcomes [5,6]. Thus we chose TGN as part of our probe to enable the probe penetrating through BBB. Beside, nucleolin is overexpressed on glioma cells [7]. Its corresponding ligand, AS1411, is a G-rich aptamer and has been utilized as targeting ligand to mediate nanoparticles target to glioma [8,9]. Taking the advantages of TGN and AS1411 together, we conjugated TGN and AS1411 for glioma imaging.

In this study, TGN and AS1411 were conjugated through a dual functional PEG linker. To track the probe, shorted as AsT, Cy3 was anchored onto the 3' end of AS1411. Several experiments, including cellular uptake, tumor spheroids uptake, ex vivo imaging and slices distribution, were carried out to evaluate the glioma targeting effect of AsT.

2. Materials and methods

2.1. Materials

AS1411, Cy3-AS1411 and TGN were synthesized by Sangon (Shanghai, China). Maleimide-polyethyleneglycol-N-hydroxy-suc-

* Corresponding authors. Tel.: +86 10 68410099.

E-mail addresses: shjwkk@sina.com, sshen@fudan.edu.cn (S. Shen), lymi75@163.com (Y. Liu).

¹ These two are the first authors having given equal contribution.

cinimide (MAL-PEG-NHS) was purchased from Seebio Biotech, Inc. (Shanghai, China). C6, U87, BG2, A549, HUVEC and Raw246.7 cell lines were purchased from the Institute of Biochemistry and Cell Biology, Shanghai Institutes for Biological Sciences, Chinese Academy of Sciences (Shanghai, China). bEnd.3 cell line was purchased from American type culture collection (ATCC) (VA, USA). Dulbecco's Modified Eagle Medium (high glucose) cell culture medium (DMEM) and FBS were purchased from Life Technologies (NY, USA). Cell culturing dishes and plates were purchased from Wuxi NEST Biotechnology Co. Ltd. (Wuxi, China). Rabbit anti-nucleolin antibody was purchased from Abcam (Hong Kong, China). Alexafluor 488-conjugated donkey anti rabbit antibody was purchased from Jackson ImmunoResearch Laboratories, Inc. (PA, USA). Western blot related reagents were purchased from Beyotime (Haimen, China).

BALB/c mice (male, 4–5 weeks, 18–22 g) were obtained from Dashuo Bio technology Co., Ltd. (Chengdu, China) and maintained under standard housing conditions. All animal experiments were carried out in accordance with protocols evaluated and approved by the ethics committee of Sichuan University.

2.2. AsT synthesis and characterization

AS1411 was functionalized with TGN utilizing Maleimide-PEG-NHS as a linker (Fig. 1). Ten OD of 5' NH₂ modified AS1411 was added with 254 µg of Maleimide-PEG-NHS in 1 mL pH 8.0 PBS and stirred 3 h for conjugation. After changed the pH of PBS from 8.0 to 7.0, the mixture was added with 66 µg TGN and stirred another 24 h for the TGN conjugation. Cy3 modified AsT (Cy3-AsT) was prepared as above except 5' NH₂ modified AS1411 changed to 5' NH₂ and 3' Cy3 modified AS1411. To characterize the conjugation, production was applied to ¹H NMR using a 400 MHz spectrometer (Varian, CA, USA). Fourier transform infrared spectroscopy (FTIR) was also used to characterize the AsT. Additionally, 0.5% agarose gel electrophoresis was used to further determine the conjugation of AS1411 with TGN.

2.3. Nucleolin expression

C6, HUVEC, bEnd.3, BG2, Raw246.7, U87 and A549 cells were lysed using RPMI buffer containing 1 mM PMSF. The protein concentration was determined using the BCA method. Equivalent amounts of protein were boiled for 5 min in loading buffer and then separated by 10% SDS polyacrylamide gel electrophoresis. Proteins were transferred to nitrocellulose membranes. The membranes were blocked for 1 h in TBS containing 4% low-fat milk. Membranes were then probed with specific antibodies recognizing

the target proteins, and the proteins were visualized using an ECL reagent.

2.4. Cell uptake of AsT

C6 glioma cells and bEnd.3 cells were seeded into 24-well plates at the density of 10⁴ per 400 µL/well. One day later, 1 OD/mL Cy3-AsT or Cy3-AS1411 was added to cells and incubated for 1 h. After washed by ice-cold PBS for three times, the fluorescence intensity was observed by fluorescent microscopy (Leica, Germany).

2.5. Three dimension tumor spheroid uptake

To prepare three dimensions tumor spheroids, C6 cells were seeded at a density of 2 × 10³ cells/400 µL per well in 48-well plates coated by 150 µL 2% low melting-temperature agarose [10]. Seven days after cell seeded, tumor spheroids were added with Cy3-AsT or Cy3-AS1411 at a concentration of 1 OD/mL. After 4 or 8 h incubation, spheroids were rinsed with ice-cold PBS for three times and fixed by 4% paraformaldehyde for 30 min. Then the spheroids were transferred to glass slides and fluorescent intensity was observed by confocal microscopy (SP5, Leica, Germany).

To determine the dual targeting effect of AsT, bEnd.3 cells were seeded in 24-well Transwell membrane at a density of 2 × 10⁴ cells/200 µL per well. Transendothelial electrical resistance (TEER) was detected by an epithelial voltammeter (Millicel-RES, Millipore, USA) to evaluate the cell monolayer integrity. Monolayers with TEER over 200 Ω/cm² were used for further experiment. Three dimensions tumor spheroids were prepared as above. Six days later, bEnd.3 monolayers contained Transwell were transferred to the 48-well plate that cultured C6 spheroids and co-cultured for another one day. One OD/mL of Cy3-AsT or Cy3-AS1411 were added into the Transwell and incubated for 8 h. Then the spheroids were rinsed and fixed. The fluorescent intensity was observed by confocal microscopy (SP5, Leica, Germany).

2.6. Ex vivo imaging and tissue distribution

Glioma bearing mice were established as described previously [11]. Mice were anesthetized and 5 µL suspension containing 5 × 10⁵ C6 cells was injected into the right corpus striatum of the mice. Ten days later, 300 OD/kg of Cy3-AsT or Cy3-AS1411 were i.v. injected into the glioma bearing mice. Two hours later, mice were sacrificed and perfused. Then the tissues were sampled and the distribution of fluorescence was observed by an IVIS

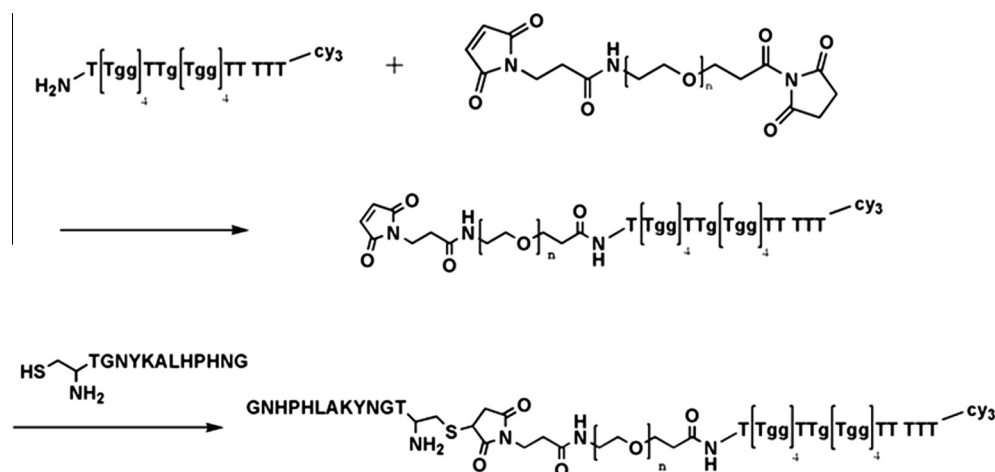


Fig. 1. Synthesis route of AsT.

spectrum in vivo imaging system (Caliper, MA, USA). After fixed with 4% paraformaldehyde overnight, the tissues were dehydrated for preparing frozen section with 10 μm thicknesses. Nucleon was stained with rabbit anti-nucleolin antibody followed with Alexa-fluor 488-conjugated goat anti-rabbit IgG according to previous established procedure [12]. Slices of normal tissue were stained with 0.5 $\mu\text{g}/\text{mL}$ of DAPI. The distribution of fluorescence was observed by a confocal microscope (TCS SP5, Leica, Germany).

3. Results and discussion

3.1. Characterization of AsT

^1H NMR of TGN showed an adsorption at 1.34 ppm with three peaks (Fig. 2A), owing to thiol in the end of TGN. After conjugation, the adsorption migrated to 1.78 ppm with four peaks (Fig. 2B), suggesting the TGN was successfully conjugated with PEG. In FTIR result (Fig. 2C), the following vibrations were observed: stretching vibrations of N–H at 3440 cm^{-1} , and stretching vibrations of C=O

at 1643 cm^{-1} , indicating the formation of amide. The synthesized AsT was further evaluated by electrophoresis. AS1411 could effectively migrate to positive electrode because of its negative charge. Physical mixture of AS1411 and TGN also displayed migration, indicating AS1411 was independent in the physical mixture. However, AsT was still in the origin position, which was because the conjugation possessed higher molecular weight and lower charge intensity, indicating the AS1411 successfully modified onto TGN.

3.2. Cell uptake

The expression of nucleolin in different kinds of cells was determined by Western blot (Fig. 3A). The expression of nucleolin on C6 glioma cells was high, while the expression on bEnd.3 cells was much lower, which was consistent with previous studies [7,13]. Thus C6 cells were used to determine the glioma targeting efficiency of AS1411 and AsT, and bEnd.3 cells were used to represent brain endothelial cells. In vitro, C6 cells could uptake both AS1411 and AsT at similar intensity (Fig. 3B), owing to the targeting ability

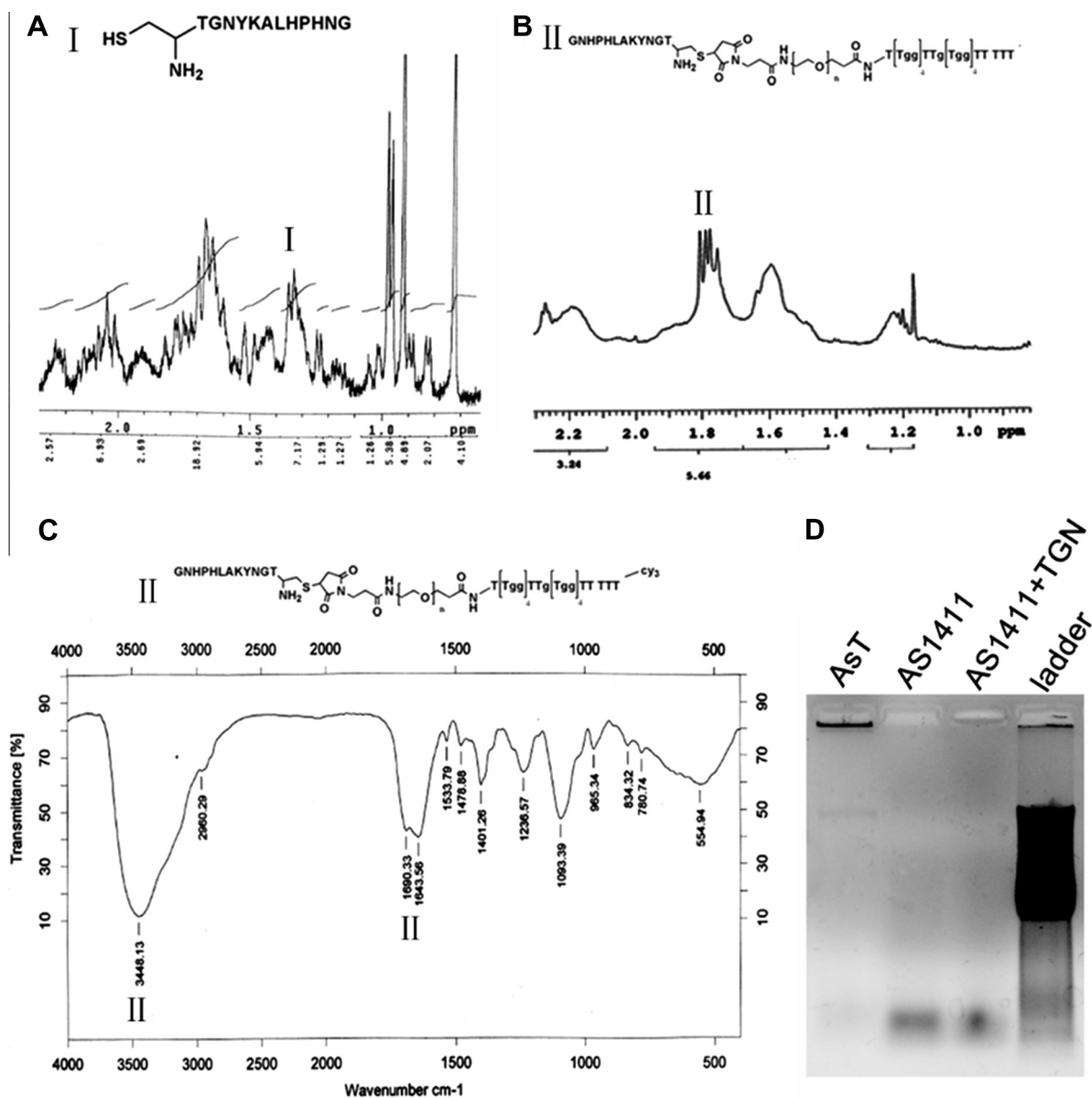


Fig. 2. (A) ^1H NMR of TGN-SH. (B) ^1H NMR of AsT. (C) FTIR of AsT. (D) Agarose gel electrophoresis of AsT, using AS1411 and the mixture of AS1411 and TGN as control.

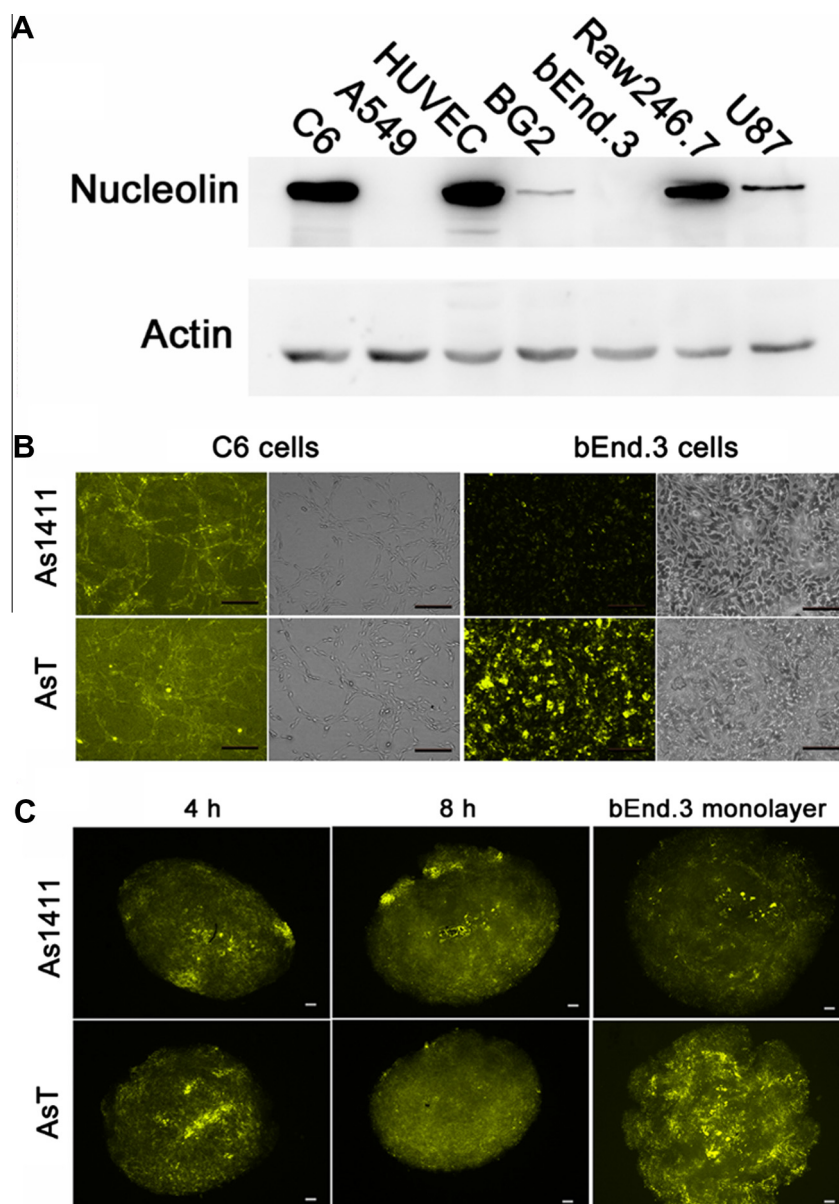


Fig. 3. (A) Expression of nucleolin in various cells. (B) C6 and bEnd.3 cells uptake of Cy3-AS1411 and Cy3-AsT at equal AS1411 concentration for 1 h. Bar represents 50 μ m. (C) Cy3-AS1411 and Cy3-AsT uptake by C6 tumor spheroids with or without bEnd.3 monolayers for 8 h. Bar represents 50 μ m.

of AS1411 [14]. However, the uptake of AsT by bEnd.3 cells was significantly higher than that of AS1411, owing to the endothelial cell targeting ability of TGN [5]. These results demonstrated AsT could target to both glioma cells and endothelial cells, which was useful for in vivo glioma imaging.

3.3. Tumor spheroids uptake

Tumor spheroids are sufficient models for in vitro evaluation of penetrating ability of both nanoparticulated systems and small molecules because of not only the convenient establishment procedure but also the similar microenvironment to in vivo tumors such as high inner pressure, low O_2 , low pH, etc. [15,16]. After 4 h and 8 h incubation, both AS1411 and AsT could penetrate into the spheroids (Fig. 3C). However, after cocultured with bEnd.3 monolayers, the fluorescent intensity of spheroid that incubated with AS1411 was much lower than that of AsT, suggesting the modification of TGN enabled the AsT to penetrate through bEnd.3 monolayers and uptake by C6 spheroid [17]. While without TGN,

AS1411 could be prevented by the monolayers from reaching and taking up by the C6 spheroids. In combination, the results demonstrated both AS1411 and TGN were essential for completely conquering the two barriers faced by glioma imaging and targeting to glioma cells.

3.4. Ex vivo imaging

Ex vivo imaging results showed poor intensity of AS1411 in brain glioma, owing to the prevention by BBB [18]. While the intensity of AsT was much higher than that of AS1411, which demonstrated AsT was more effective probe for glioma imaging because of its dual targeting capacity (Fig. 4A). Tissue slices were prepared to further evaluate the targeting efficiency of AsT and AS1411. In nucleolin positive glioma cells, there were obviously higher intensity of AsT compared to AS1411, which was consistent with in vitro tumor spheroids study (Fig. 4B). Additionally, the distribution in normal tissues was slightly altered. These results strongly demonstrated AsT could be used as an effective probe for glioma imaging (Fig. 4C).

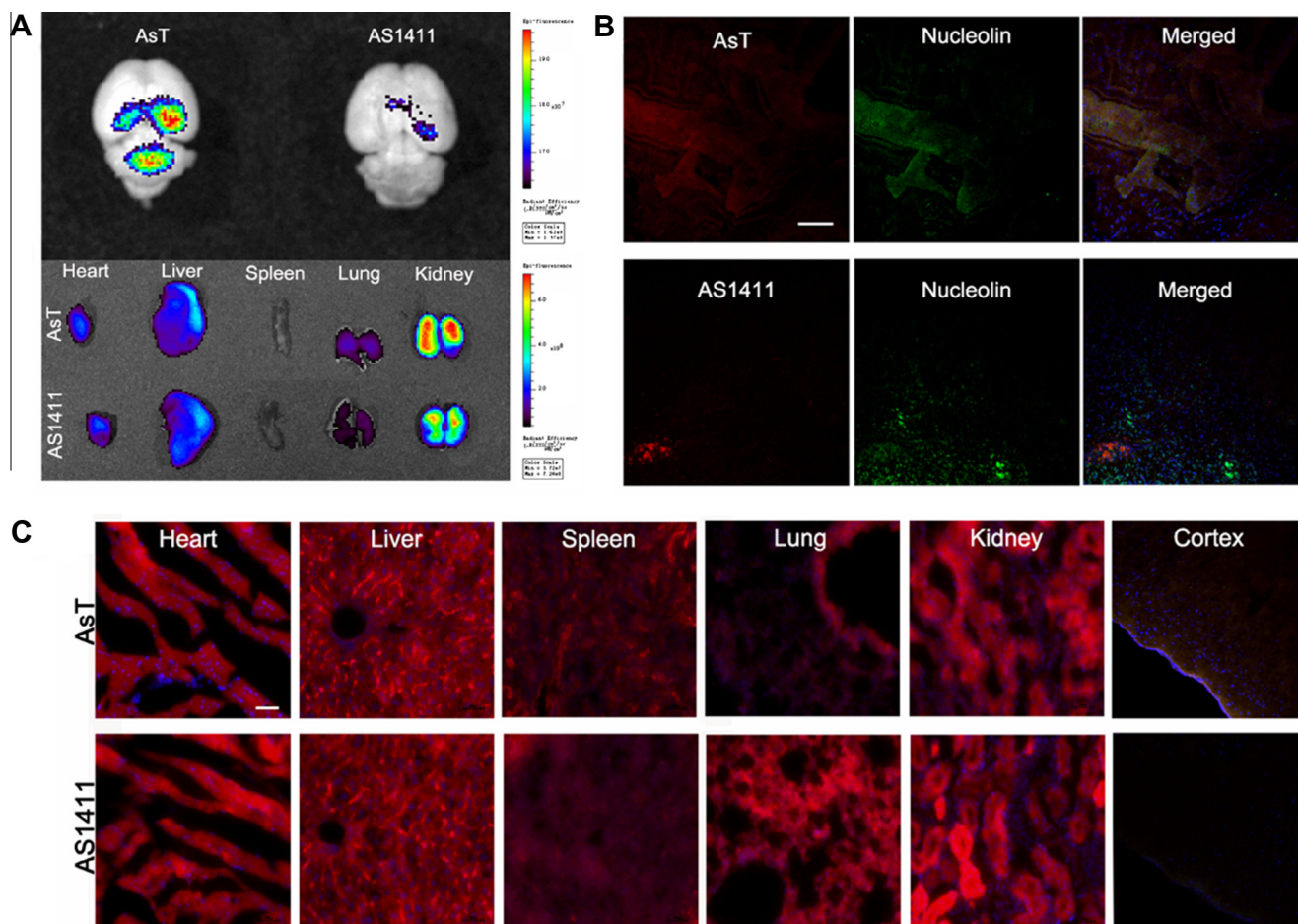


Fig. 4. (A) Ex vivo imaging of glioblastoma bearing mice administrated with Cy3-AS1411 or Cy3-AsT. (B) Distribution of AsT and AS1411 in nucleolin-positive glioma cells. Bar represents 100 μ m. (C) Distribution of AsT and AS1411 in normal tissues. Blue represents nuclei and bar represents 100 μ m. (For interpretation of the references to color in this figure legend, the reader is referred to the web version of this article.)

In our study, AsT was successfully synthesized, which could target both glioma cells and endothelial cells, showing obviously better glioma imaging capacity.

References

- [1] S. Agarwal, R. Sane, R. Oberoi, J.R. Ohlfest, W.F. Elmquist, Delivery of molecularly targeted therapy to malignant glioma, a disease of the whole brain, *Expert Rev. Mol. Med.* 13 (2011) e17.
- [2] J. Clarke, N. Butowski, S. Chang, Recent advances in therapy for glioblastoma, *Arch. Neurol.* 67 (3) (2010) 279–283.
- [3] Q.T. Nguyen, E.S. Olson, T.A. Aguilera, T. Jiang, M. Scadeng, L.G. Ellies, et al., Surgery with molecular fluorescence imaging using activatable cell-penetrating peptides decreases residual cancer and improves survival, *Proc. Natl. Acad. Sci. U.S.A.* 107 (9) (2010) 4317–4322.
- [4] H. Gao, Z. Pang, X. Jiang, Targeted delivery of nano-therapeutics for major disorders of the central nervous system, *Pharm. Res.* 30 (10) (2013) 2485–2498.
- [5] J. Li, L. Feng, L. Fan, Y. Zha, L. Guo, Q. Zhang, et al., Targeting the brain with PEG-PLGA nanoparticles modified with phage-displayed peptides, *Biomaterials* 32 (21) (2011) 4943–4950.
- [6] C. Zhang, X. Wan, X. Zheng, X. Shao, Q. Liu, Q. Zhang, et al., Dual-functional nanoparticles targeting amyloid plaques in the brains of Alzheimer's disease mice, *Biomaterials* 35 (1) (2014) 456–465.
- [7] A.G. Hovanesian, C. Soundaramourty, K.D. El, I. Nondier, J. Svab, B. Krust, Surface expressed nucleolin is constantly induced in tumor cells to mediate calcium-dependent ligand internalization, *PLoS ONE* 5 (12) (2010) e15787.
- [8] J. Guo, X. Gao, L. Su, H. Xia, G. Gu, Z. Pang, et al., Aptamer-functionalized PEG-PLGA nanoparticles for enhanced anti-glioma drug delivery, *Biomaterials* 32 (31) (2011) 8010–8020.
- [9] H. Gao, J. Qian, S. Cao, Z. Yang, Z. Pang, S. Pan, et al., Precise glioma targeting of and penetration by aptamer and peptide dual-functioned nanoparticles, *Biomaterials* 33 (20) (2012) 5115–5123.
- [10] H. Gao, J. Qian, Z. Yang, Z. Pang, Z. Xi, S. Cao, et al., Whole-cell SELEX aptamer-functionalised poly(ethyleneglycol)-poly(epsilon-caprolactone) nanoparticles for enhanced targeted glioblastoma therapy, *Biomaterials* 33 (26) (2012) 6264–6272.
- [11] S. Jones-Bolin, H. Zhao, K. Hunter, A. Klein-Szanto, B. Ruggeri, The effects of the oral, pan-VEGF-R kinase inhibitor CEP-7055 and chemotherapy in orthotopic models of glioblastoma and colon carcinoma in mice, *Mol. Cancer Ther.* 5 (7) (2006) 1744–1753.
- [12] H. Gao, S. Pan, Z. Yang, S. Cao, C. Chen, X. Jiang, et al., A cascade targeting strategy for brain neuroglial cells employing nanoparticles modified with angiopep-2 peptide and EGFP-EGF1 protein, *Biomaterials* 32 (33) (2011) 8669–8675.
- [13] S. Christian, J. Pilch, M.E. Akerman, K. Porkka, P. Laakkonen, E. Ruoslahti, Nucleolin expressed at the cell surface is a marker of endothelial cells in angiogenic blood vessels, *J. Cell Biol.* 163 (4) (2003) 871–878.
- [14] C.R. Ireson, L.R. Kelland, Discovery and development of anticancer aptamers, *Mol. Cancer Ther.* 5 (12) (2006) 2957–2962.
- [15] F. Perche, N.R. Patel, V.P. Torchilin, Accumulation and toxicity of antibody-targeted doxorubicin-loaded PEG-PE micelles in ovarian cancer cell spheroid model, *J. Control. Release* 164 (1) (2012) 95–102.
- [16] M.T. Santini, G. Rainaldi, Three-dimensional spheroid model in tumor biology, *Pathobiology* 67 (3) (1999) 148–157.
- [17] H. Gao, Z. Yang, S. Zhang, Z. Pang, Q. Liu, X. Jiang, Study and evaluation of mechanisms of dual targeting drug delivery system with tumor microenvironment assays compared with normal assays, *Acta Biomater.* 10 (2) (2014) 858–867.
- [18] C. Zhan, W. Lu, The blood-brain/tumor barriers: challenges and chances for malignant gliomas targeted drug delivery, *Curr. Pharm. Biotechnol.* 13 (12) (2012) 2380–2387.